



the society for solid-state
and electrochemical
science and technology

Journal of The Electrochemical Society

Enhanced Red Phosphorescence in $\text{MgGeO}_3\text{:Mn}^{2+}$ by Addition of Yb^{3+} Ions

Yan Cong, Bin Li, Shumei Yue, Liming Zhang, Wenlian Li and Xiao-jun Wang

J. Electrochem. Soc. 2009, Volume 156, Issue 4, Pages H272-H275.
doi: 10.1149/1.3077570

Email alerting service

Receive free email alerts when new articles cite this article - sign up in the box at the top right corner of the article or [click here](#)

To subscribe to *Journal of The Electrochemical Society* go to:
<http://jes.ecsdl.org/subscriptions>

© 2009 ECS - The Electrochemical Society



Enhanced Red Phosphorescence in $\text{MgGeO}_3\text{:Mn}^{2+}$ by Addition of Yb^{3+} Ions

Yan Cong,^{a,b} Bin Li,^{a,z} Shumei Yue,^a Liming Zhang,^{a,b} Wenlian Li,^a and Xiao-jun Wang^{c,*}

^aKey Laboratory of Excited State Processes, Changchun Institute of Optics, Fine Mechanics and Physics, Chinese Academy of Sciences, Changchun, 130033, China

^bGraduate School of the Chinese Academy of Sciences, Chinese Academy of Sciences, Beijing, 100039, China

^cDepartment of Physics, Georgia Southern University, Statesboro, Georgia 30460, USA

Enhancement of the ${}^4\text{T}_{1\text{g}}({}^4\text{G}) \rightarrow {}^6\text{A}_{1\text{g}}({}^6\text{S})$ red emission of $\text{MgGeO}_3\text{:1\% Mn}^{2+}$ with addition of Yb_2O_3 is reported. The initial phosphorescence in the Yb_2O_3 codoped sample is an order of magnitude stronger than that of the Yb_2O_3 -free sample. Thermoluminescence spectra indicate that the introduction of Yb^{3+} into the host produces traps with a suitable depth, resulting in the enhanced red phosphorescence of Mn^{2+} . The possible mechanism for this phenomenon is explained by a competitive trapping model.

© 2009 The Electrochemical Society. [DOI: 10.1149/1.3077570] All rights reserved.

Manuscript submitted October 13, 2008; revised manuscript received January 8, 2009. Published February 9, 2009.

Long-lasting phosphorescence (LLP) materials have long been of interest for various displays and signing applications.^{1–4} Blue and green oxide persistent phosphors, such as $\text{Sr}_4\text{Al}_{14}\text{O}_{25}\text{:Dy,Eu}$,⁵ $\text{SrAl}_2\text{O}_4\text{:Dy,Eu}$,¹ exhibiting high brightness of phosphorescence with better chemical stability over sulfides are commercially available. However, commercial red-emitting oxide-persistent phosphors with a long persistence time have not yet been obtained.

Manganese ions ($3d^5$ configuration) should be expected as an efficient activator for red long persistent phosphors due to their highly efficient luminescence and broad emissive range from 490 to 750 nm in a different host. Many studies on the luminescence behaviors of the Mn^{2+} activator have been reported.^{6–9} The $3d^5$ multiplet energies of Mn^{2+} in crystals depend largely on the covalency interaction with the host crystal or the crystal field, because the 3d electrons of the transition metal ions are the outermost ones. The octahedral coordinated Mn^{2+} ion exhibits orange to red emissions.¹⁰

Generally, either intrinsic or foreign defects are harmful to luminescent efficiency of activators because they could compete with activators and trap the excitation energy through nonradiative transitions.¹¹ The density of traps plays a key role in the persistent emission of phosphor materials.³ To improve the phosphorescence intensity and persistent time, the introduction of defects induced by adding auxiliary activators is needed.^{1,12} In this article, the red phosphorescence enhancement of $\text{MgGeO}_3\text{:Mn}^{2+}$ by codoping Yb^{3+} into the phosphor is reported. The initial phosphorescence intensity in the codoped sample is 1 order of magnitude higher than that of the Yb^{3+} -free sample, and the persistent time is prolonged from several minutes to 30 min.

Experimental

Sample preparation.—The Mn^{2+} -doped MgGeO_3 phosphors were prepared using the traditional solid-state reaction method. Analytical grade GeO_2 , MgO , $\text{C}_4\text{H}_6\text{MnO}_4 \cdot 4\text{H}_2\text{O}$, and Yb_2O_3 were used as starting materials. Those mixed-powder materials were homogenized, thoroughly ground with an agate pestle in an agate mortar, and then sintered at 1250°C for 3 h using alumina crucibles with alumina lids in air atmosphere.

Analysis and measurements.—The X-ray diffraction (XRD) data were collected by a Rigaku D/max-IIIB X-ray powder diffractometer using $\text{Cu K}\alpha 1$ ($\lambda = 0.15405$ nm) radiation. The energy-

dispersive X-ray spectrum (EDX) result was observed by a HITACHI-4800 scanning electron microscope equipped with an EDX.

The photoluminescence (PL) and excitation spectra as well as phosphorescence decay curves were measured on a Hitachi F-4500 fluorescence spectrophotometer equipped with a 150 W Xenon lamp as the excitation source. The phosphorescence was measured after irradiation by 254 nm UV light for 5 min. The thermoluminescence (TL) spectra were recorded by heating the irradiated samples from room temperature to 250°C using the FJ-427A TL meter (Beijing Nuclear Instrument Factory) with a fixed heating rate at 2°C/s . All the measurements were carried out at room temperature except for the TL spectra.

Results and Discussion

Phase characterizations.—The XRD patterns of $\text{MgGeO}_3\text{:1\% Mn}^{2+}$ singly doped and $\text{MgGeO}_3\text{:Mn}^{2+},\text{Yb}^{3+}$ codoped samples are shown in Fig. 1a. It is clearly indicated that the samples are chemically and structurally single-phased MgGeO_3 , which corresponds to the JCPDS (no. 34-0281). There are no extra peaks observed in the XRD pattern from the Yb_2O_3 -added sample, suggesting that Yb^{3+} is well incorporated into MgGeO_3 lattice. The ionic radii of Yb^{3+} ($r = 0.093$ nm) is closer to that of Mg^{2+} ($r = 0.072$ nm) than that of Ge^{4+} ($r = 0.053$ nm); thus, we believe that Yb^{3+} ions prefer to occupy the Mg^{2+} sites. The inset of Fig. 1a shows a blueshift of the XRD peaks in the Yb codoped sample compared to the Yb-free sample, which can be attributed to the lattice expansion because the ionic radii of Yb^{3+} is larger than that of Mg^{2+} . Therefore, the blueshift provides the evidence of the Yb^{3+} incorporation into MgGeO_3 lattices, and the Yb^{3+} should substitute for the Mg^{2+} . The EDX result as shown in Fig. 1b also confirms the presence of Yb in the $\text{MgGeO}_3\text{:Mn}^{2+},\text{Yb}^{3+}$ codoped sample, which indicate Yb^{3+} ions are incorporated into $\text{MgGeO}_3\text{:Mn}^{2+}$ more clearly.

PL properties of $\text{MgGeO}_3\text{:Mn}^{2+}$ phosphor.—The excitation and emission spectra of $\text{MgGeO}_3\text{:0.01 Mn}^{2+}$ are presented in Fig. 2a. The emission spectrum exhibits a red emission band at 650 nm, originating from ${}^4\text{T}_{1\text{g}}({}^4\text{G}) \rightarrow {}^6\text{A}_{1\text{g}}({}^6\text{S})$ transition of Mn^{2+} with an excitation at 254 nm.¹³ A blue emission band centered at 400 nm is attributed to the host. The excitation spectrum monitoring the 650 nm emission consists of a broadband centered at 254 nm and two shoulder bands centered at 209 and 238 nm, respectively. The band centered at 254 nm is due to the transition of Mn^{2+} [${}^6\text{A}_{1\text{g}}(\text{S}) \rightarrow {}^4\text{A}_{1\text{g}}(\text{F})$], and the two shoulders are related to the absorption of the host. In order to explain the emission and excitations related to the host, an undoped MgGeO_3 sample was also synthesized. As shown in Fig. 2b, two peaks centered at 209 and 238 nm,

* Electrochemical Society Active Member.

^z E-mail: lib020@ciomp.ac.cn; xwang@georgiasouthern.edu

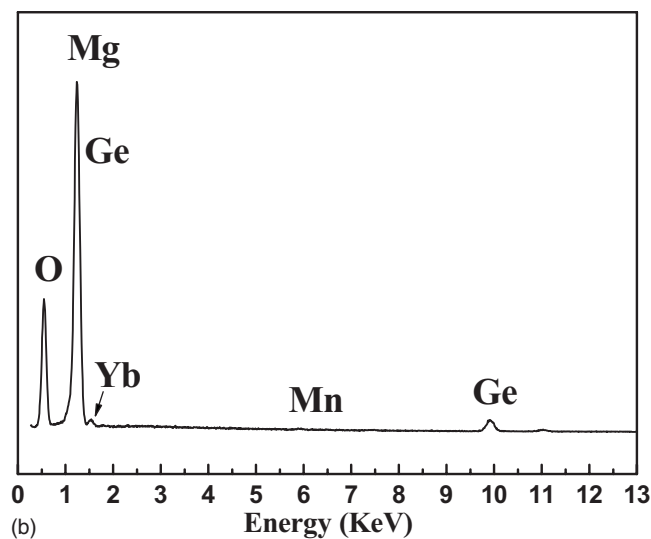
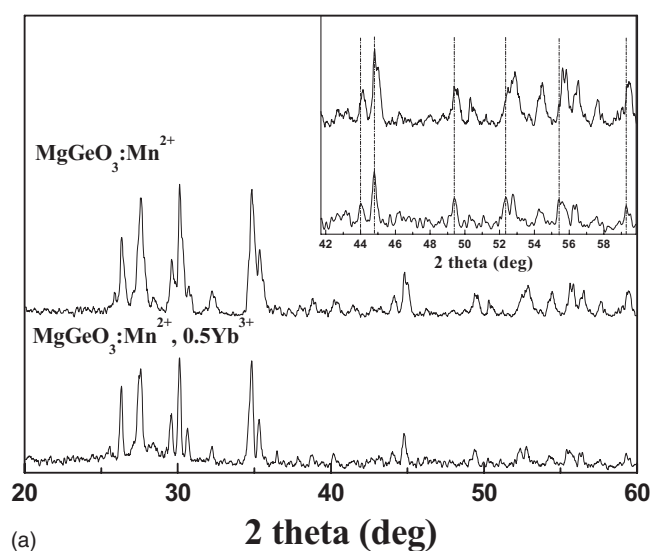


Figure 1. Powder XRD patterns of MgGeO_3 : (a) Mn^{2+} and MgGeO_3 : Mn^{2+} , Yb^{3+} and (b) EDX for MgGeO_3 : Mn^{2+} , Yb^{3+} .

respectively, are presented in the excitation spectrum and a broad-band emission peaked at 400 nm on the excitations is observed. The results indeed indicate that 209 and 238 nm excitations belong to the host absorption, and therefore, the MgGeO_3 is a self-activated material.

In addition, the excitation at 254 nm for the Mn^{2+} doped sample overlaps with the host emission band. An intensity decrease of the host emission at 400 nm on 238 nm excitation is observed compared to that of the Mn^{2+} -doped sample, suggesting a possible energy transfer from the host to the Mn^{2+} ions.

Effect of Yb_2O_3 on the phosphorescence properties of MgGeO_3 : Mn^{2+} .—After removal of excitation source, the MgGeO_3 : Mn^{2+} sample yields weak red LLP. The introduction of Yb_2O_3 greatly improves the red LLP performance but weakens the PL intensity of Mn^{2+} . Figure 3 depicts the dependence of PL intensity (empty bars) and initial phosphorescence intensity (shaded bars) on Yb^{3+} concentration in the codoped sample. The PL intensity in the samples decreases after Yb_2O_3 is incorporated into the host. The defects introduced by Yb^{3+} quench the PL of Mn^{2+} . However, the defects act as traps to substantially improve the phosphorescence. As shown in Fig. 3, the phosphorescence from the Yb_2O_3 codoped samples appears more intense than that from the Yb_2O_3 free

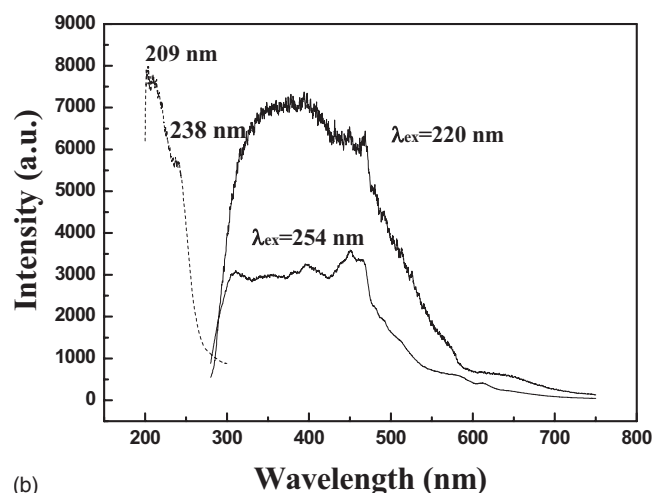
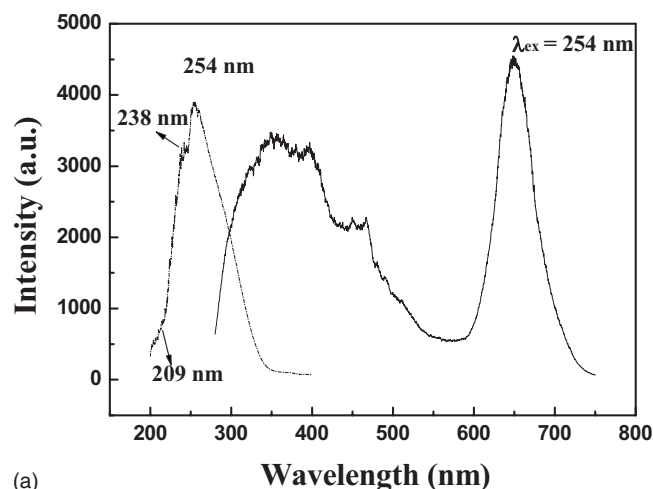


Figure 2. Excitation and emission spectra of (a) MgGeO_3 :0.01 Mn^{3+} and (b) undoped MgGeO_3 samples.

samples. The maximum of the phosphorescence intensity happens at the Yb^{3+} concentration of 0.5%, which is 1 order of magnitude higher than that in the Yb_2O_3 free sample.

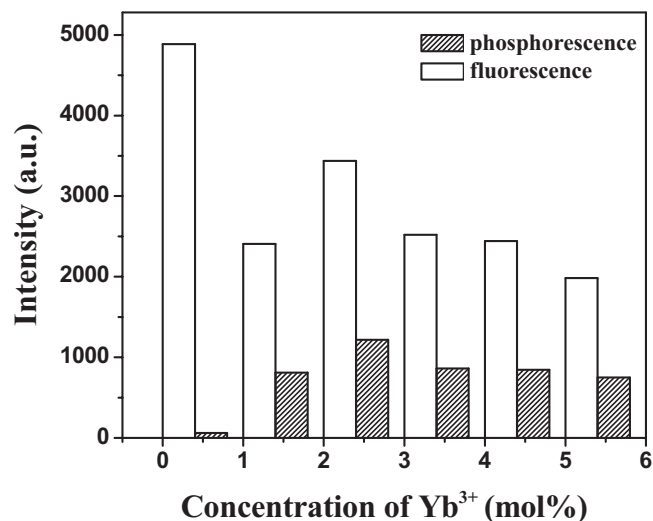


Figure 3. Dependence of luminescence intensities (empty bars) and initial phosphorescence intensities (shaded bars) on Yb^{3+} concentration in MgGeO_3 : Mn^{2+} , $x\text{Yb}^{3+}$ ($x = 0, 0.1, 0.5, 1.0, 2.0, 5.0$).

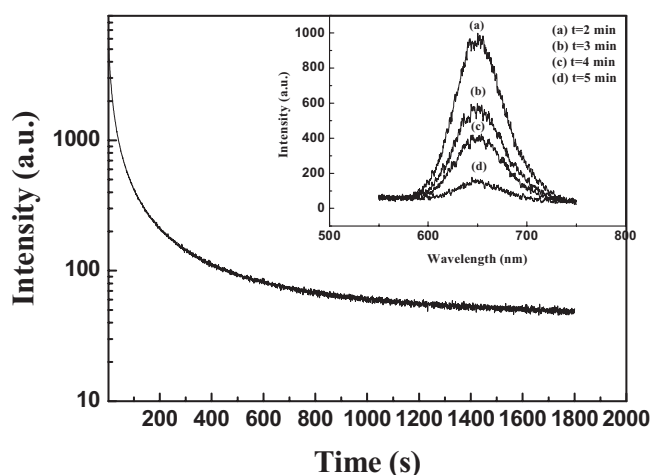


Figure 4. Afterglow intensity decay curve of the $\text{MgGeO}_3:1\% \text{Mn}^{2+}$, $0.5\% \text{Yb}^{3+}$ phosphor. The inset patterns are the afterglow spectra of phosphor after the excitation source is switched off at different times (2, 3, 4, and 5 min).

Figure 4 illustrates the time decay curve of phosphorescence in $\text{MgGeO}_3:1 \text{ mol } \% \text{Mn}^{2+}$, $0.5 \text{ mol } \% \text{Yb}^{3+}$ after irradiation with 254 nm UV light for 2 min. The persistent time is prolonged from several minutes to 30 min. The electron storage capacity of persistent phosphors is related to the trap depth and concentration. The Yb^{3+} -doped sample produces more defects that greatly enhance the phosphorescence. As shown in the inset of Fig. 4, the afterglow spectra are recorded at different times (at 2, 3, 4, and 5 min, respectively) after the excitation source is switched off. It is found that the center (650 nm) and the profile of the red LLP emission remain unchanged and are consistent with PL emission under steady excitation. It is indicated that both LLP and PL result from the same ${}^4\text{T}_{1g} \rightarrow {}^6\text{A}_{1g}$ transition of Mn^{2+} .

TL measurements are also performed in order to characterize the traps. The TL spectra of Mn^{2+} singly doped and $\text{Mn}^{2+}\text{Yb}^{3+}$ codoped samples are shown in Fig. 5. For the $\text{MgGeO}_3:\text{Mn}^{2+}$, one broad thermal peak is observed at 133°C , formed by charge defects created by substituting Mg^{2+} by Mn^{2+} , which corresponds to the trap depth of 0.69 eV calculated using the variable heating rate method proposed by Hoogenstraaten.¹⁴ For the Yb^{3+} codoped sample, beside the peak at 133°C , an additional thermal peak at 44°C is observed, corresponding to the trap (depth of the trap is 0.55 eV) in-

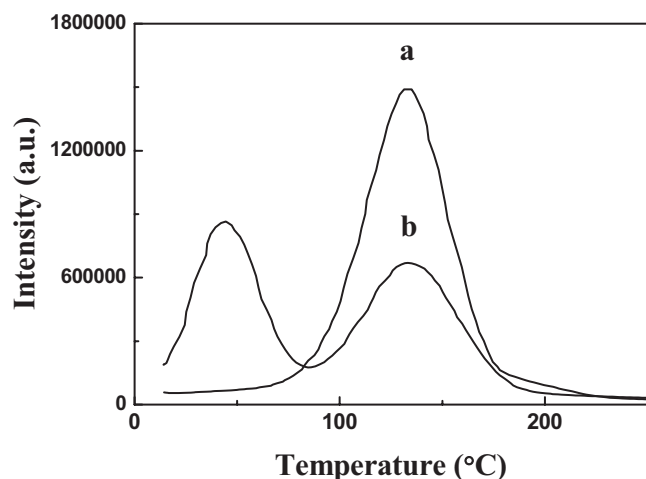


Figure 5. TL spectra of (a) Yb^{3+} free and (b) $0.5 \text{ mol } \% \text{Yb}^{3+}$ ions-doped $\text{MgGeO}_3:\text{Mn}^{2+}$ samples.

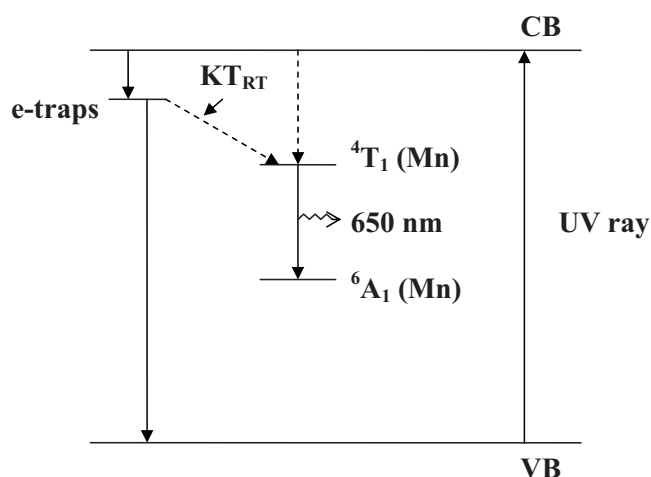


Figure 6. Possible process of the red LLP in the $\text{MgGeO}_3:\text{Mn}^{2+}$ phosphor.

roduced by Yb^{3+} . For LLP material, one critical factor is the suitable trap depth correlated to the TL peaks.^{15,16} The optimized peak is situated slightly above room temperature for better LLP performance. The LLP process will be dominated by the corresponding traps.^{1,17,18} Therefore, the peak at 44°C due to the electron traps created by Yb^{3+} is responsible for the improvement of red LLP of Mn^{2+} .¹⁹

Possible mechanism of the LLP of $\text{MgGeO}_3:\text{Mn}^{2+}, \text{Yb}^{3+}$.— The LLP is due to the thermally stimulated recombination of holes and electrons that are trapped at the metastable states at room temperature.²⁰ On the basis of the above TL curves and the PL spectra result, it should be thought that one energy transfer from the host to the Mn^{2+} ions favors to create the LLP. It can be assumed that free electrons and holes in the sample are generated under UV excitation. The holes are captured by Mn^{2+} ions, which form the excited state of Mn^{2+} ions. The Mg^{2+} substitution by Mn^{2+} creates appropriate traps or oxygen vacancies associated with Ge^{4+} ions, where electrons are captured.²¹ One part of the trapped electrons was released by heat at room temperature and turned back to the valence band, giving blue emission. This process has been approved by the PL of the undoped phosphor as shown in Fig. 2b. The majority of electrons stored in the electron traps transfers to the excited state of Mn^{2+} ions.⁶ Finally, the excited state of Mn^{2+} ions decay radiatively into the ground state with the red phosphorescence due to the ${}^4\text{T}_1 \rightarrow {}^6\text{A}_1$ transition resulting in red LLP of Mn^{2+} . The mechanism of the phosphorescence can be formulated in detail using a simplified scheme as shown in Fig. 6.

However, the electron traps depth is deepish because its relative temperature of TL peak is high at 133°C as shown in Fig. 5. The electrons are captured by the traps with deep depth, leading to poor performance of red LLP of Mn^{2+} for several minutes. As the conclusion in the XRD results, when the trivalent Yb ions are codoped in the host matrix, the Yb^{3+} ions tend to substitute for Mg^{2+} ions rather than Ge^{4+} because the ionic radii of Yb^{3+} ($r = 0.093 \text{ nm}$) is closer to that of Mg^{2+} ($r = 0.072 \text{ nm}$) than that of Ge^{4+} ($r = 0.053 \text{ nm}$). Yb^{3+} ions replacing Mg^{2+} ions produces Yb_{Mg}' defects with negative charge to maintain the electroneutrality of the phosphors. This negative Yb_{Mg}' site impurity traps with relative TL peak at 44°C , produced by codoped Yb^{3+} , is preferred as the electron trap with suitable depth. In the codoped sample, the amount of the defects located at 133°C decreases greatly, and most electrons are captured by the defects with suitable depth instead of the deeper defects, resulting in improvement of red LLP performance of Mn^{2+} .

Conclusion

Enhancement of red emission in $\text{MgGeO}_3:\text{Mn}^{2+}$ phosphor has been obtained with addition of Yb_2O_3 . Influences of the excess Yb^{3+} ions and introduced defects on red PL and LLP of the phosphor have been systematically investigated. The TL spectra approve that the introduction of Yb^{3+} into the host produces traps with suitable depth, resulting in enhanced red phosphorescence of Mn^{2+} . The possible mechanisms of phosphorescence have been discussed.

Acknowledgments

The authors gratefully thank the financial support of the One Hundred Talents Project from the Chinese Academy of Sciences and the National Natural Science Foundation of China (grants no. 20571071, no. 50872130, and no. 10574128).

Chinese Academy of Sciences assisted in meeting the publication costs of this article.

References

1. T. Matsuzawa, Y. Aoki, N. Takeuchi, and Y. Matsuzawa, *J. Electrochem. Soc.*, **143**, 2670 (1996).
2. J. Qiu, K. Miura, and H. Inouye, *Appl. Phys. Lett.*, **73**, 1763 (1998).
3. D. Jia, R. S. Meltzer, W. M. Yen, W. Jia, and X. J. Wang, *Appl. Phys. Lett.*, **80**, 1535 (2002).
4. M. Kowatari, D. Koyama, Y. Satoh, K. Linuma, and S. Uchida, *Nucl. Instrum. Methods Phys. Res. A*, **480**, 431 (2002).
5. M. Wang, D. Wang, and G. Lu, *Mater. Sci. Eng., B*, **57**, 18 (1998).
6. B. Lei, Y. Liu, Z. Ye, and C. Shi, *J. Lumin.*, **109**, 215 (2004).
7. B. Lei, B. Li, X. Wang, and W. Li, *J. Lumin.*, **118**, 173 (2006).
8. C. R. Ronda and T. Amrein, *J. Lumin.*, **69**, 245 (1996).
9. L. E. Shea, R. K. Datta, and J. J. Brown, *J. Electrochem. Soc.*, **141**, 1950 (1994).
10. D. T. Palumbo and J. J. Brown, *J. Electrochem. Soc.*, **117**, 1184 (1970).
11. W. V. Schaik and G. Blasse, *Chem. Mater.*, **4**, 410 (1992).
12. D. Jia, X. J. Wang, and W. M. Yen, *Chem. Phys. Lett.*, **363**, 241 (2002).
13. T. Sanada, K. Yamamoto, K. Kojima, and N. Wada, *J. Sol-Gel Sci. Technol.*, **41**, 237 (2007).
14. W. Hoogenstraaten, *Philips Res. Rep.*, **13**, 515 (1958).
15. D. Haranath, V. Shanker, H. Chander, and P. Sharma, *Mater. Chem. Phys.*, **78**, 6 (2002).
16. A. Nag and T. R. N. Kutty, *J. Alloys Compd.*, **354**, 221 (2003).
17. J. Wang, S. Wang, and Q. Su, *J. Solid State Chem.*, **177**, 895 (2004).
18. Y. Liu, B. Lei, and C. Shi, *Chem. Mater.*, **17**, 2108 (2005).
19. M. Yamazaki and K. Kojima, *Solid State Commun.*, **130**, 637 (2004).
20. J. Qiu, K. Miura, H. Inouye, S. Fujiwara, T. Mitsuyu, and K. Hirao, *J. Non-Cryst. Solids*, **244**, 185 (1999).
21. M. Iwasaki, D. N. Kim, K. Tanaka, T. Murata, and K. Morinaga, *Sci. Technol. Adv. Mater.*, **4**, 137 (2003).